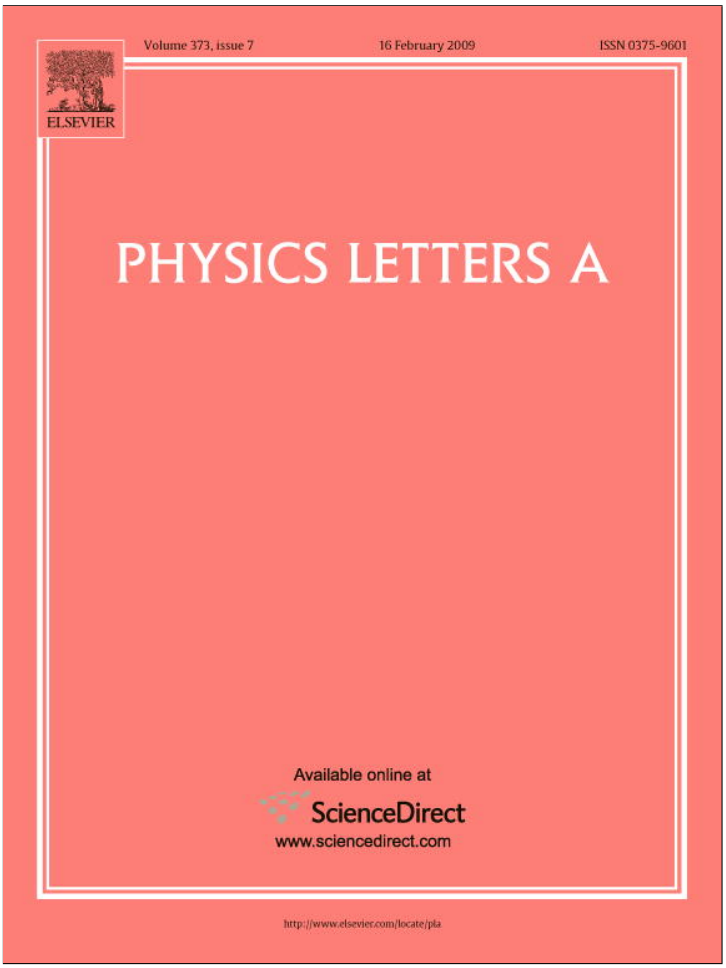

Physics Letters A 373 (2009) 769–772

Contents lists available at ScienceDirect

Physics Letters A

www.elsevier.com/locate/pla

Single-chain dynamics of linear polyethylene liquids under shear flow

J.M. Kim, B.J. Edwards *, D.J. Keffer, B. Khomami

Department of Chemical and Biomolecular Engineering, University of Tennessee, Knoxville, TN 37996, USA

ARTICLE INFO

Article history:
Received 1 August 2008
Received in revised form 27 October 2008
Accepted 29 December 2008
Available online 7 January 2009
Communicated by F. Porcelli

PACS:
61.20.Ja
61.20.Gy
61.25.Hq

Keywords:
Nonequilibrium molecular dynamics
Reptation theory
Rotational motion

ABSTRACT

Molecular dynamics simulations of linear $C_{78}H_{158}$ were conducted to investigate the dynamics of individual chains under shear. The distribution of the end-to-end vector exhibited Gaussian behavior at low shear rates; however, it displayed a bimodal form at high shear rates as rotational motion of the individual chains effectively lowered the vector's magnitude. Correlations between the components of the end-to-end vector revealed multiple time scales associated with the fluid response: the Rouse time, and several that were associated with the deformation and rotational dynamics of the fluid.

Mechanistic insight into the dynamics of individual macromolecules comprising polymeric liquids is of critical importance to the development of hi-fidelity models for describing the rheological and morphological properties of these complex fluids under flow. Reptation-based molecular theories are currently the primary tool for describing the microstructural and rheological properties of entangled linear polymer melts. These theories are based on the concept that chain molecules move like a snake in a contorted tube formed by the surrounding molecules. Although the original reptation-based model for linear polymer melts of Doi and Edwards [1] has deficiencies, recent advances in reptation theories have resolved some long-standing issues with respect to the model's ability to describe the nonlinear rheology of entangled linear polymers [2]. Specifically, the most comprehensive versions of recent theories perform well in describing subtle details of the rheology of entangled polymers at low shear rates; i.e., smaller than the inverse of the reptation time scale, which is the time required for a representative chain to disengage from its original tube. Further success has been achieved at intermediate shear rates, which are larger than the inverse of the reptation time but smaller than the inverse of the Rouse time that governs tube stretching [3,4]. At the high shear rates typical of many processing operations, agreement with the most sophisticated molecular theories has been only partial, and has consistently been shown to diverge from experiment [5].

The physics of linear polyethylene chains at high shear rates is examined in this Letter. Although the liquid studied, $C_{78}H_{158}$, is of insufficient length to constitute an entangled system, it is still useful to understand this (short-chain) limit of linear polymer chain behavior. By analyzing this behavior over a range of shear rates and chain lengths, a thorough understanding of entry into the entangled regime can be obtained [6]. Hence the examination of the high-shear dynamics of this short-chain system might aid the ultimate resolution of the same issue in highly entangled polymers.

Recent direct visualization using video microscopy provided the first experimental glimpse of single-chain dynamics under shear [5]. Clearly, this class of experiments is extremely important in developing the mechanistic insight required for the development of advanced molecular theories of strong flows. However, performing experiments over a broad configuration space for various types of flow is a very challenging and time-consuming task. Furthermore, the primary limitation lies in the small number of polymer chains that can be examined in this way.

Atomistic simulations offer a complementary perspective from which to study individual chains and their configurational distributions over a broad range of flow types and strengths. Simulations offer the possibility to investigate the dynamics of each chain within the test fluid. This allows much more detailed information to be gleaned from simulation with respect to the experiment, as statistically meaningful correlations can be established via averaging of the single-chain dynamical behavior. Prior simulations

* Corresponding author.
E-mail address: bje@utk.edu (B.J. Edwards).

0375-9601/$ – see front matter
doi:10.1016/j.physleta.2008.12.062

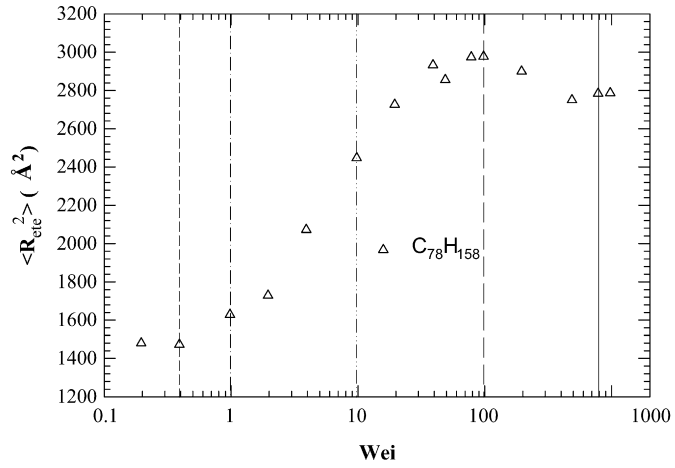

Fig. 1. $\langle R^2_{\text{ete}} \rangle$ vs. *Wei* for $C_{78}H_{158}$ under shear.

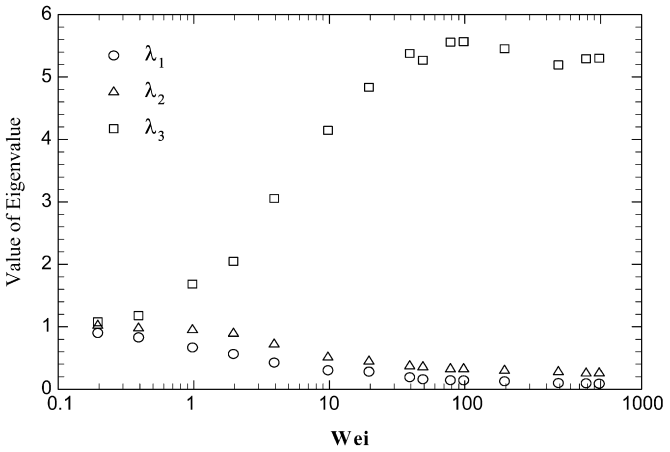

Fig. 2. Eigenvalues of $\tilde{\mathbf{C}}$ as functions of *Wei*.

of chain liquids focused on obtaining the bulk rheological and topological properties of these fluids [6–10], and did not explicitly examine the dynamics of individual molecules. In this Letter, the simulation analysis is extended to encompass the dynamical behavior of each molecule within the fluid, thus allowing determination of statistically meaningful correlations between individual chain configurations and dynamics. Of particular interest are correlations of the components of the end-to-end vector at high shear rates.

Nonequilibrium molecular dynamics simulations of linear polyethylene $C_{78}H_{158}$ were carried out in the *NVT* ensemble using the united atom model of Siepmann et al. [11]. This model has been used extensively for simulating rheological behavior of alkanes and polyethylenes, and specific values of the parameters, as assigned in the present simulations, may be found in Refs. [7,8].

The simulation encompassed 160 molecules of $C_{78}H_{158}$. The simulation box was constructed with dimensions (130.50, 54.00, 54.00) Å in (x, y, z) space, and the density of $C_{78}H_{158}$ was set at 0.7640 g/cm^3. The temperature was maintained at 450 K over the course of each simulation. At equilibrium, the simulation revealed a Rouse relaxational time (τ_R) of 2 300 ps, fitting an exponential KWW function [12,13] to the autocorrelation of the trace of the dyad of $\mathbf{R}_{\text{ete}}$. All relevant details concerning the implementation of the shear flow simulations can be found in recent articles [7,8]. Under a homogenous shear field of magnitude $\dot{\gamma}$, the simulation volume was oriented such that x was the direction of flow, y the gradient direction, and z the neutral direction.

The mean-square, end-to-end chain distance, $\langle R^2_{\text{ete}} \rangle$, is grossly correlated with the atomistic configurations of the constituent chain molecules, and is an important quantification variable in many kinetic theory models of polymeric fluid dynamics. However, its use is most often predicated on convenient, yet theoretically unjustifiable, pre-averaging or closure approximations, which largely ignore the dynamics of individual macromolecules. Fig. 1 displays $\langle R^2_{\text{ete}} \rangle$ as a function of the Weissenberg number ($Wei = \dot{\gamma}\tau_R$) for the model fluid. Note that $Wei = 1$ is associated with the boundary between Newtonian and shear-thinning viscosity behaviors under shear, as verified by prior simulations [7–9]. Initially, there is a rapid rise in the magnitude of the end-to-end vector with increasing *Wei*, as expected; however, at a critical *Wei* of about 100, $\langle R^2_{\text{ete}} \rangle$ attains a maximum value of 2 978 Å^2, and then decreases with *Wei*. Note that the chains are not completely elongated, since the fully-extended value of $\langle R^2_{\text{ete}} \rangle$ is 9 890 Å^2 [8]. Fig. 2 presents the Eigenvalues of the conformation tensor,

$$\tilde{\mathbf{C}} = \frac{3\langle \mathbf{R}_{\text{ete}} \mathbf{R}_{\text{ete}} \rangle}{\langle R^2_{\text{ete}} \rangle}, \tag{1}$$

as functions of *Wei*. The primary Eigenvalue quantifies the stretch contribution to the data of Fig. 1, and the secondary and tertiary Eigenvalues emphasize the high degree of molecular stretching at high shear. These two Eigenvalues also imply a high degree of orientation, on average, with respect to the flow direction. The counter-intuitive behavior associated with the primary Eigenvalue mirrors the behavior displayed in Fig. 1, since the trace of $\mathbf{R}_{\text{ete}}\mathbf{R}_{\text{ete}}$ is dominated by the stretching contribution.

This counter-intuitive behavior is correlated with a minimum and subsequent increase in the intermolecular Lennard–Jones (LJ) energy of the system with increasing shear rate [8,9]. Moore et al. [9] hypothesized that this effect was due to the competition between flow-induced forces, which tend to stretch and orient the chains, and Brownian-like collisional forces which tend to randomize the chain configurations. From their perspective, the mechanistic response of the chain at low shear rates is dominated by the orientational and stretching forces induced by the surrounding flow field; however, as the shear rate increases, the kinetic energy of the constituent atomic units eventually becomes great enough to allow an effective competition between the stretching force of the flow and the randomizing collisional force. This competition leads to the minimum in the LJ curve as the collisional forces begin to dominate the response of the individual chains.

In this Letter, an alternative hypothesis to the one described above is proposed. Here, the maximum in the $\langle R^2_{\text{ete}} \rangle$ curve occurs in response to the development of substantial rotational motion of the individual chains, which effectively lowers the magnitude of the ensemble average value of $\langle R^2_{\text{ete}} \rangle$: when a chain is rotating, its end-to-end vector has a smaller magnitude on a time-averaged basis than when it remains stretched and oriented at some angle relative to the applied shear field.

Fig. 3 displays data for the probability distribution function (PDF) with respect to $|\mathbf{R}_{\text{ete}}|$, the end-to-end vector's magnitude, for five values of *Wei* that correspond to the vertical lines in Fig. 1. At the lowest values of *Wei*, the behavior of the PDF is decidedly Gaussian, as expected; i.e., the PDF is dominated by a single peak, centered symmetrically around the average value of $|\mathbf{R}_{\text{ete}}|$. The system response is effectively governed solely by the Rouse time, which is congruent with most pre-averaged rheological theories. However, contrary to the pre-averaged rheological theories, the distribution decreases in height and increases in width as *Wei* increases from 0.39 to 0.98, although both distributions remain essentially Gaussian. In pre-averaged theories, the distributions become more peaked with increasing *Wei*, and also become narrower. This behavior is caused by the greater stretching and orientation of the chains with increasing *Wei*, which is the only effective mechanism of chain deformation in these theories. The broadening of

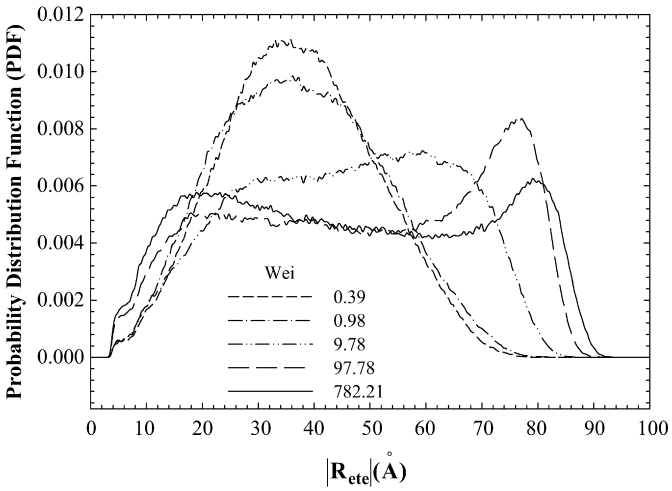

Fig. 3. Probability distribution vs. $|\mathbf{R}_{ete}|$.

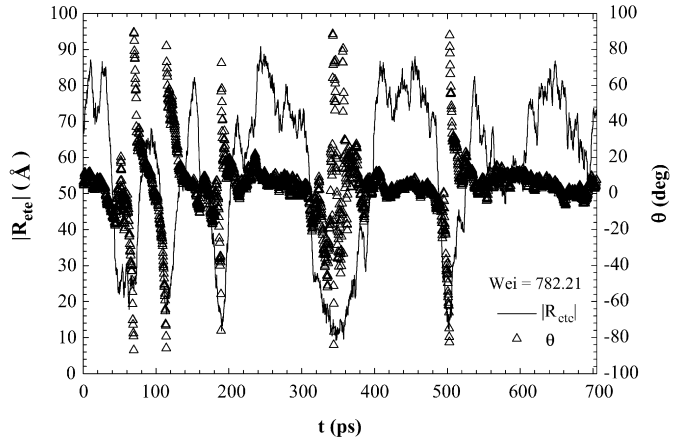

Fig. 4. $|\mathbf{R}_{ete}|$and θ vs. time for a chain.

the distribution indicates a failure of pre-averaging approximations.

As *Wei* increases to unity, the peak of the distribution moves to higher values of $|\mathbf{R}_{ete}|$, as expected, but the distribution has grown considerably in width. At higher values of *Wei*, the distribution has become decidedly bimodal, with the stretch peak at high $|\mathbf{R}_{ete}|$ being balanced by the formation of another peak at low $|\mathbf{R}_{ete}|$. As expounded below, the lower $|\mathbf{R}_{ete}|$ peak is correlated with the rotation or tumbling of the chain molecules under shear. As *Wei* increases, more of the molecules rotate on average, and with greater frequencies, such that the average value of $|\mathbf{R}_{ete}|$ is effectively smaller than it would be were no tumbling to occur. As *Wei* increases, the stretch peak decreases in magnitude, although it continues to move to higher values of $|\mathbf{R}_{ete}|$. The rotational peak grows with increasing *Wei* as the tumbling frequency of the chains continues to increase.

Although this tumbling of the molecular chains was observed most recently in dilute solutions [5,14,15], it is very different from that observed here. In the dilute solutions, the chains rotate freely at higher frequencies and with a more circular motion than observed in the PE simulations. Furthermore, the bimodality of the distribution provides evidence that at least two distinct processes are vying for dominance of the chains' dynamics.

Fig. 4 displays simulation data for $|\mathbf{R}_{ete}|$ and the orientation angle, θ, of $\mathbf{R}_{ete}$ with respect to the direction of flow for a random chain molecule of the simulation. This figure depicts the rotational motion of a single chain with time, for which $|\mathbf{R}_{ete}|$ varies from

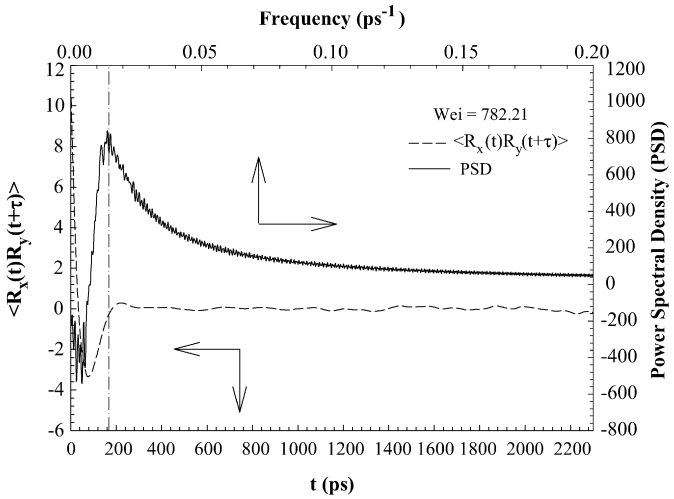

Fig. 5. $\langle R_x(t)R_y(t+\tau)\rangle_\tau$ vs. τ and PSD vs. frequency.

a tightly coiled configuration to nearly a fully extended chain (of length 99.45 Å). These dramatic changes in $|\mathbf{R}_{ete}|$ are correlated with corresponding behavior of θ. The orientation angle clearly shows a semi-periodic tumbling of the chain molecules, and the sudden rotations of θ directly affect $|\mathbf{R}_{ete}|$ in that the chain ends pass each other very closely, causing a substantial reduction of the average chain length associated with the tumbling motions. Note that the tumbling of the chains can be followed by relatively long periods of dormancy, as evidenced in Fig. 4. On time average, each chain will take on a positive orientation with respect to the direction of flow; however, Brownian fluctuations will often induce chain orientations in the negative direction, at which point tumbling may occur due to the highly compressive apparent force in the adverse direction. Most rotation occurs in a highly ellipsoidal, hairpin motion; i.e., the segmental chain motion is primarily along the direction of the chain backbone, corresponding to the direction of flow and average tube orientation of about 5° at this value of the shear rate.

The mechanistic dynamics of chains can be investigated through calculation of time correlation functions for the components of $\mathbf{R}_{ete}$. This allows determination of characteristic timescales intrinsic to the dynamical chain processes. Aust et al. [14] examined time correlations of the components of the gyration tensor for a dilute polymer solution (i.e., a single chain in a sea of solvent) via NEMD simulation, and demonstrated that the average chain angular velocity approached the theoretical value of the vorticity $(-\dot{\gamma}/2)$ as $\dot{\gamma} \to 0$. As the shear rate increased, the chain became increasingly elongated and its angular velocity dropped relative to the vorticity of the shear field [14].

In Fig. 5, data for the correlation $\langle R_x(t)R_y(t+\tau)\rangle_\tau$ are presented with respect to observation time at $Wei = 782$, wherein the subscript τ indicates time integration up to this limit. Note that $\langle R_x(t)R_x(t+\tau)\rangle_\tau$ and $\langle R_y(t)R_y(t+\tau)\rangle_\tau$ displayed the same qualitative behavior as indicated in the figure, and that similar plots were obtained at all values of *Wei* investigated. These data reveal a definite correlation between certain components of $\mathbf{R}_{ete}$, with characteristic timescales that are dependent on *Wei*. These time scales are quantified using the power spectral density, also displayed in Fig. 5, through Fourier transformation of the correlation signal. Cross correlations between other off-diagonal pairs of components revealed no correlations. With respect to the dynamics of $\mathbf{R}_{ete}$, it is evident that the correlations describe various aspects of the dynamics of the rotational motion of the chains.

Fig. 6 displays data for the intrinsic timescales associated with the dynamical chain motion: τ_R, the Rouse time, as well as τ_{xx}, τ_{xy},

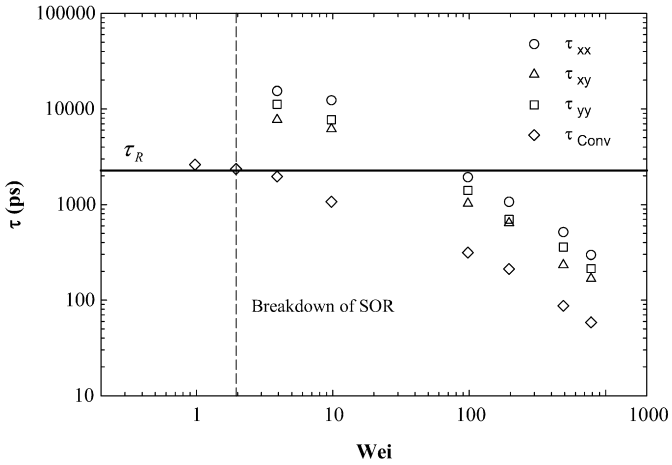

Fig. 6. The times τ_R, τ_{xx}, τ_{xy}, τ_{yy}, and τ_{conv} vs. *Wei*.

τ_{yy}, and τ_{conv}, as functions of *Wei*. The τ_{ii} are associated with the correlations of the corresponding components of $\mathbf{R}_{\text{ete}}$, as defined above. The timescales are associated with various aspects of the chain rotation, such as the tumbling frequency, wagging motion, etc. The timescale τ_{conv} is assumed to be associated with a form of configurationally dependent relaxation time [16], and is defined by assuming that the $R_x R_x$ correlation bears the functional form of $A\exp(-t/\tau_{\text{conv}})\cos(2\pi t/\tau_{xx})$, where A is a constant. At equilibrium, $\tau_{xx} \to \infty$, so that $\tau_{\text{conv}} \to \tau_R$. As $\tau_{\text{conv}} \to \infty$, the motions of the chains are purely tumbling, similarly to rigid rods.

As *Wei* decreases from high shear rates toward the low shear regime ($Wei < 2$), the τ_{ii} increase as the system becomes increasingly isotropic (assuming values 5–10 times τ_R), and the mechanistic response of the chains is governed more by Brownian fluctuations and configurational deformation processes than by the kinematics of the flow. Decreasing shear to $Wei = 2$, these timescales vanish from the correlation profiles, and the only timescale that remains in this regime is τ_R. Note that this value of *Wei* corresponds to the profile in Fig. 3 where the distribution became non-Gaussian. Consequently, as discussed prior, the rotational dynamics of the chain appear to be dominated by the configurational and Brownian processes in the linear shear regime.

Increasing values of *Wei* beyond 2, the timescales τ_{ii} are reduced dramatically, until they have decreased below the Rouse time, indicating a higher frequency of tumbling and resulting in the first peak in the bimodal distributions of Fig. 3. Thus at high shear rates ($Wei > 100$), the rotational motion of the chains dominates the system response. The timescale τ_{conv} is equivalent to τ_R at low shear rates, but then also decreases substantially at higher shear rates. This quantifies the affect of the kinematics on the convection and orientation of the chain configurations within the fluid; i.e., as the chains become stretched to their maximum lengths and uniformly oriented in the direction of flow, they form highly oriented parallel network structures, which allow freer rotation of neighboring chains. The data presented in Fig. 6 indicate that the low shear response appears to be dominated by the elasticity associated with chain configurational entropy, and the high shear response is dominated by the vorticity of the flow.

The polyethylene chains examined with these simulations are obviously of insufficient length to possess a significant entangled network structure. Nevertheless, under low shear, the chain dynamics appear to be governed by well understood entropically elastic behavior, whereas the flow kinematics (i.e., the local fluid vorticity) at high shear appear to dictate the chain dynamics. This might be associated with a significant amount of alignment and stretching at higher *Wei*, as is evident in Figs. 1–3: as the shear rate increases, more cylindrical structures of less tortuosity are formed, allowing freer rotational motion of the chain molecules. Furthermore, the transition zone between the two flow regimes correlates well with the critical strain rate for the breakdown of the stress-optical law; i.e., $Wei = 2$ [17]. Hence the onset of chain tumbling might play a critical role in the breakdown of this law.

Acknowledgements

This work was supported by the National Science Foundation under Grant No. CBET-0742679. Partial computational support was provided by the *National Center for Supercomputing Applications*.

References

[1] M. Doi, S.F. Edwards, The Theory of Polymer Dynamics, Clarendon Press, Oxford, 1986.
[2] R.G. Larson, The Structure and Rheology of Complex Fluids, Oxford Univ. Press, Oxford, 1999.
[3] V. Mhetar, L.A. Archer, J. Polym. Sci.: Polym. Phys. 38 (2000) 222.
[4] M.T. Islam, J. Sanchez-Reyes, L.A. Archer, Rheol. Acta 42 (2003) 191.
[5] R.E. Teixeira, A.K. Dambal, D.H. Richter, E.S.G. Shaqfeh, S. Chu, Macromol. 40 (2007) 2461.
[6] J.M. Kim, D. Keffer, M. Kröger, B.J. Edwards, J. Non-Newtonian Fluid Mech. 152 (2008) 168.
[7] C. Baig, B.J. Edwards, D.J. Keffer, H.D. Cochran, J. Chem. Phys. 122 (2005) 184906.
[8] C. Baig, B.J. Edwards, D.J. Keffer, H.D. Cochran, J. Chem. Phys. 124 (2006) 084902.
[9] J.D. Moore, S. Cui, H.D. Cochran, P.T. Cumings, J. Non-Newtonian Fluid Mech. 93 (2000) 83.
[10] R. Khare, J.J. de Pablo, J. Chem. Phys. 107 (1997) 6956.
[11] J.I. Siepmann, S. Karaborni, B. Smit, Nature 365 (1993) 330.
[12] K. Kohlrausch, Pogg. Ann. Phys. Chem. 91 (1854) 56.
[13] G. Williams, D.C. Watts, Trans. Faraday Soc. 66 (1970) 80.
[14] C. Aust, S. Hess, M. Kröger, Macromol. 35 (2002) 8621.
[15] C.M. Schroeder, R.E. Teixeira, E.S.G. Shaqfeh, S. Chu, Phys. Rev. Lett. 95 (2005) 018301.
[16] A. Souvaliotis, A.N. Beris, J. Rheol. 36 (1992) 241.
[17] C. Baig, B.J. Edwards, D.J. Keffer, Rheol. Acta 46 (2007) 1171.